

Evolutionary Paths Underlying Flower Color Variation in *Antirrhinum*

Annabel C. Whibley,^{1*} Nicolas B. Lenglade,^{1*} Christophe Andalo,² Andrew I. Hanna,³ Andrew Bangham,³ Christophe Thébaud,² Enrico Coen^{1†}

To understand evolutionary paths connecting diverse biological forms, we defined a three-dimensional genotypic space separating two flower color morphs of *Antirrhinum*. A hybrid zone between morphs showed a steep cline specifically at genes controlling flower color differences, indicating that these loci are under selection. *Antirrhinum* species with diverse floral phenotypes formed a U-shaped cloud within the genotypic space. We propose that this cloud defines an evolutionary path that allows flower color to evolve while circumventing less-adaptive regions. Hybridization between morphs located in different arms of the U-shaped path yields low-fitness genotypes, accounting for the observed steep clines at hybrid zones.

A prevalent metaphor for describing evolutionary processes is the adaptive landscape, commonly visualized in three dimensions as an undulating surface of fitness values over a two-dimensional (2D) space representing various genotypes (1, 2). Different species may be considered to be at separate peaks on the landscape or to lie along ridges of high fitness. The notion of peaks is favored by the incompatible adaptive features of species, whereas ridges are favored as a way of accounting for underlying adaptive continuity. More recently, it has been argued that the issue of peaks versus ridges is an artifact of low-dimensional visualizations of fitness spaces as landscapes (3). What seem like separate peaks in 3D landscapes may be connected by paths in higher dimensions: the higher the dimensionality, the more likely such connections exist. However, it has proved difficult to demonstrate these paths in nature because of the challenge of dealing with higher dimensional genotypic and phenotypic spaces. We address this issue by combining molecular, genetic, and computational approaches to analyze flower color variation in natural populations and species of *Antirrhinum*.

Southern Europe contains 17 to 28 *Antirrhinum* species and subspecies, the number depending on taxonomic criteria (4–7). Although the species display diverse morphologies and flower colors, they can be crossed with each other and with the model species *A. majus* to give fertile progeny, reflecting their recent evolutionary origin (8–10). In most cases, the species occupy nonoverlapping geographical regions, precluding natural hybridization. Hybrid zones arise where species or morphs come into

contact, as happens in a region of the Pyrenees for the yellow-flowered *A. m. striatum* and the magenta-flowered *A. m. pseudomajus* (Fig. 1A).

Previous studies on nine species from the *Antirrhinum* group identified several major loci involved in natural flower color variation (11–13). These include the linked *ROSEA* (*ROS*) and *ELUTA* (*EL*) loci, affecting the intensity and pattern of magenta anthocyanin pigment, and *SULFUREA* (*SULF*), affecting the distribution

of yellow aurone pigment. To test whether these loci were important for color differences between *A. m. striatum* and *A. m. pseudomajus*, we crossed the two morphs to *A. majus* lines of known genotype (Fig. 2A). The F1s derived from the magenta morph were all magenta. By contrast, the yellow morph failed to complement mutations in *ROS* and *SULF* (Fig. 2A). The yellow morph also gave progeny with reduced magenta pigmentation when crossed to wild type, with a pattern similar to that conferred by the dominant *EL* allele. Like *EL*, the dominant allele from the yellow morph was tightly linked to *ROS* (14) (two recombinants were recovered out of 1300 test-cross progeny). Thus, *A. m. pseudomajus* is likely *ROS el/ROS el*; *SULF/SULF*, whereas *A. m. striatum* is *ros EL/ros EL*; *sulf/sulf*.

To assess further the contribution of *ROS* *EL* and *SULF* alleles to flower color differences, we intercrossed the two morphs. F2 individuals had a range of flower colors that were scored for magenta and yellow on the basis of overall visual appearance (Fig. 2B). The distributions for color were consistent, with a single segregating locus of major effect controlling each component of flower color (Fig. 2C). Individuals with a high yellow score were

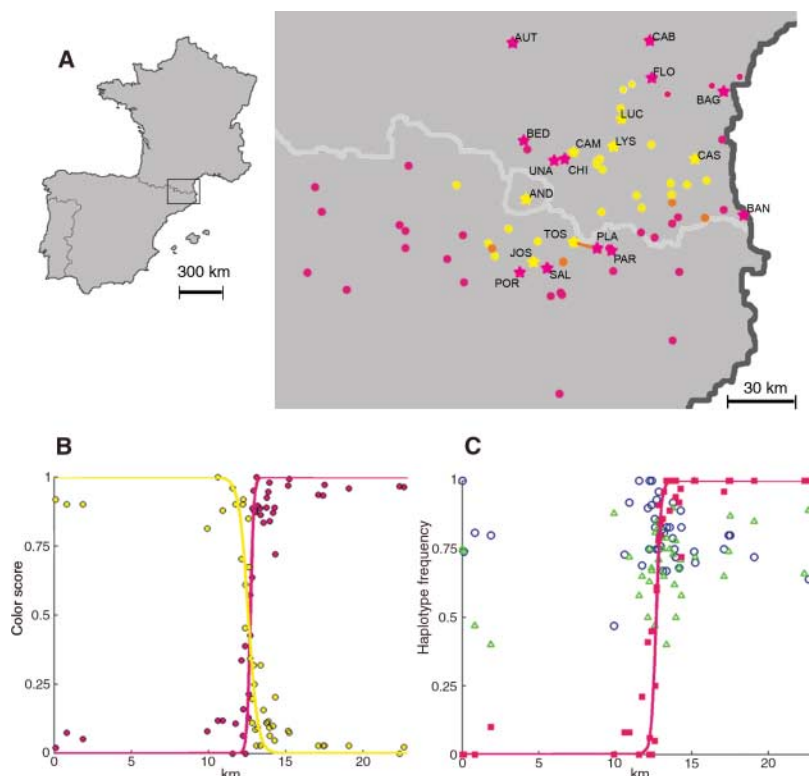


Fig. 1. Populations, phenotypes, and allele frequencies. (A) Location of the studied hybrid zone (orange line), other hybrid zones (orange circles), and sampled *A. m. pseudomajus* (magenta) and *A. m. striatum* (yellow) populations. Genetically studied populations are starred. (B) Clines in magenta and yellow color scores in subpopulations along a transect through the hybrid zone. (C) Frequencies of *ROS1* (magenta squares) and *PAL* (blue circles) haplogroups and a 6-base pair polymorphism at *DICH* (green triangles) in subpopulations along the hybrid zone transect. For *ROS1*, all markers were collapsed to a two-allele system.

¹Department of Cell and Developmental Biology, John Innes Centre, Colney Lane, Norwich NR4 7UH, UK. ²Laboratoire Evolution et Diversité Biologique, UMR 5174 CNRS–Université Paul Sabatier, 31062 Toulouse Cédex 9, France. ³School of Computing Sciences, University of East Anglia, Earlham Road, Norwich NR4 7TJ, UK.

*These authors contributed equally to this work.

†To whom correspondence should be addressed. E-mail: enrico.coen@bbsrc.ac.uk

sulf/sulf, whereas those with a low yellow score were either *SULF/SULF* or *SULF/sulf*, indicating that *SULF* genotype was the major determinant of variation in yellow. Individuals with a low magenta score were *ros EL/ros EL*, those with an intermediate score were *ROS el/ros EL*, and those with a high magenta score were *ROS el/ROS el*. Therefore, variation in magenta was largely accounted for by the *ROS EL* loci. These results allowed us to create an appropriate genotypic space for the F2. Digital images of representative flowers of four genotypes were warped to the same average flower shape. Principal component analysis on variation in pixel color at each position in the flower then allowed us to define a 3D genotypic space controlling flower color (15–17) (Fig. 2D).

The role of flower color variation in natural populations was assessed by analyzing a hybrid zone between *A. m. pseudomajus* and *A. m. striatum*. Scoring 493 plants across the hybrid zone revealed a steep cline for flower color (Fig. 1B). Allelism tests on 14 plants from the contact zone with a range of phenotypes confirmed that flower color was largely determined by *ROS*, *EL*, and *SULF* genotypes. For *ROS*, more extensive genotyping could be carried out by using molecular markers. The *ROS* locus comprises a tandem duplication of two MYB-related transcription factors, *ROS1* and *ROS2*, with *ROS1* having a greater role in flower color variation (13). We sequenced a 1.2-kb region of *ROS1*, from the promoter to the start of the second exon. Sequences from 13 yellow and 15 magenta morphs from locations distant from the contact zone showed that *ROS1* alleles fell into three major groups (haplogroups) (Fig. 3A). One haplogroup was specific to yellow morphs and was identical to the *ros^{dor}* allele of *A. majus*, hypothesized to have been derived from the wild (13). The other two haplogroups were found only in magenta morphs. *ROS1* sequences were used to design primers that allowed haplogroups to be distinguished by polymerase chain reaction. Genotyping 528 plants from the hybrid zone showed that the cline in *ROS1* haplogroup frequency coincided with magenta flower color (Fig. 1C).

Assuming that the hybrid zone arose from contact between previously separate yellow and magenta populations, the observed clines in flower color and genotype might have two explanations (18, 19). One is that *A. m. striatum* and *A. m. pseudomajus* came into recent contact and the clines reflect a neutral mixing of alleles between the populations. Alternatively, there has been a longer history of contact, and clines reflect selection maintaining morph differences. To evaluate these possibilities, we analyzed molecular variation at loci not involved in magenta and yellow morph differences. According to the neutral model, these loci should have a cline similar to that of *ROS1*. The *PALLIDA* (*PAL*) and *DICHOTOMA* (*DICH*) loci were chosen because they are linked to *ROS* [16

centimorgan (cM) and 9 cM from *ROS*, respectively], and sequences are available for primer design (20, 21). Alleles were sequenced from 18 individuals on either side of the hybrid zone. Most *PAL* alleles fell into two major haplogroups (Fig. 3B). *DICH* alleles showed little

haplogroup structure, although several DNA polymorphisms were detected. We genotyped 496 plants across the hybrid zone for the two *PAL* haplogroups and a polymorphism at *DICH*. No cline was observed for *PAL* or *DICH*, indicating that these genes were subject

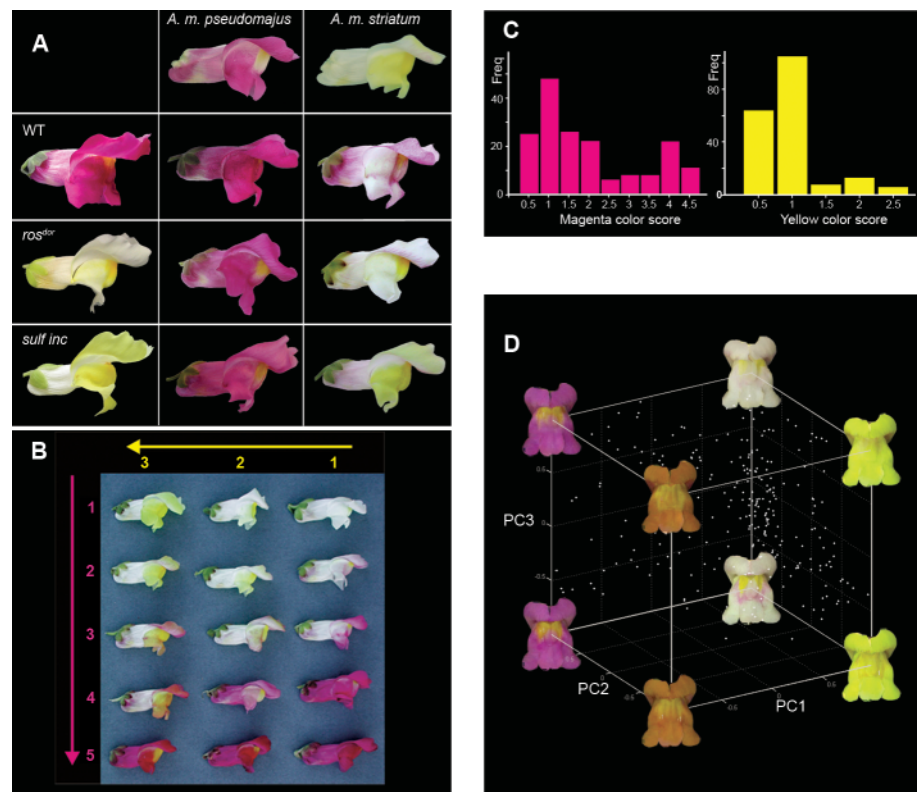


Fig. 2. Phenotypes and complementation tests. (A) F1 flowers from crosses between *A. m. pseudomajus* and *A. m. striatum* (top row) and cultivated *A. majus* genotypes (left column). *A. majus* homozygous lines are wild type (*ROS el; SULF*), *rosea^{dorsea}* (*ros^{dor} el; SULF*), and *sulfurea incolorata* (*ROS el; sulf; inc*). (B) Numerical scoring system for ranking magenta and yellow flower color. (C) Frequency of magenta (left) and yellow (right) scores in an F2 population from *A. m. striatum* × *A. m. pseudomajus*. (D) Genotypic space capturing flower color variation with three principal components (PCs). The four genotypes used for PC analysis were *ROS el/ROS el; SULF*–, *ros EL/ros EL; sulf/sulf*, *ROS el/ros EL; SULF*–, and *ros EL/ros EL; SULF*– (dash indicates unknown allele). Positions for 174 F2 and 110 F3 plants are shown as white points.

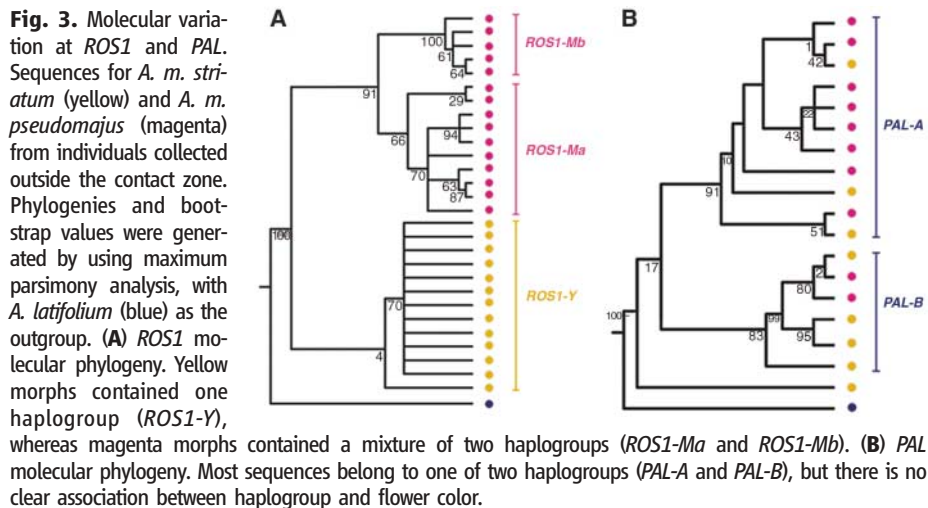


Fig. 3. Molecular variation at *ROS1* and *PAL*. Sequences for *A. m. striatum* (yellow) and *A. m. pseudomajus* (magenta) from individuals collected outside the contact zone. Phylogenies and bootstrap values were generated by using maximum parsimony analysis, with *A. latifolium* (blue) as the outgroup. (A) *ROS1* molecular phylogeny. Yellow morphs contained one haplogroup (*ROS1-Y*), whereas magenta morphs contained a mixture of two haplogroups (*ROS1-Ma* and *ROS1-Mb*). (B) *PAL* molecular phylogeny. Most sequences belong to one of two haplogroups (*PAL-A* and *PAL-B*), but there is no clear association between haplogroup and flower color.

to different evolutionary factors than *ROSI* (Fig. 1C). This was also supported by genotyping 16 *A. m. striatum* and *A. m. pseudomajus* populations distant from the hybrid zone (Fig. 1A and table S1). In all cases, the *ROSI* haplogroup correlated with flower color, whereas *PAL* and *DICH* loci showed no such association.

The simplest interpretation of these results is that spatial variation in *PAL* and *DICH* allele frequencies reflects historical gene flow between populations, whereas the *ROSI* cline has been maintained by selection on flower color. The cline could be maintained, for example, if intermediate genotypes have lower fitness than the parental morphs (22). Thus, magenta and yellow morphs might represent distinct peaks

on an adaptive landscape, whereas intermediate forms represent an intervening low fitness valley. However, this raises the problem of how the low fitness valley was traversed when the two morphs diverged from a common ancestor.

To address this issue, we mapped the range of phenotypes exhibited by *Antirrhinum* species within the defined genotypic space (Fig. 2D). This was achieved by photographing several flowers from each species (Fig. 4A) and warping the images to the same flower shape (Fig. 4B). We then determined the position in the genotypic space that best approximated the color for each flower (Fig. 4C). The approximation was evaluated by warping the resulting image back to the initial flower shape and comparing it to the original image (Fig. 4D). Much of the var-

iation in flower color was captured within the 3D genotypic space, consistent with previous studies showing that the *ROS*, *EL*, and *SULF* loci play important roles in color variation in the species group as a whole (11–13) (Fig. 4E).

When flowers from 19 species were mapped into the genotypic space, they collectively formed a broad U-shaped cloud of points (Fig. 4, F to H). Flowers from each species formed smaller clusters within this broader cloud. Magenta *A. m. pseudomajus* flowers localized near one end of the cloud, whereas yellow *A. m. striatum* flowers were near the other end. Intermediate positions within the cloud corresponded to various other patterns and intensities of color. However, certain color combinations were excluded from the cloud, even though they were observed in F2 and hybrid zone populations. For example, orange flowers, having a broad spread of both yellow and magenta (*ROS el/ROS el; sulf/sulf*), were not within the cloud (Fig. 4F). The absence of this genotype in wild species could be explained if individuals with orange flowers have lower fitness, perhaps because they are less attractive to pollinators (23–25). The role of pollinators in propagating *A. m. pseudomajus* and *A. m. striatum* is likely to be of central importance because the species are self-incompatible, seed dispersal is limited (involving gravity or water runoff), and individuals typically survive for only 1 to 3 years.

Taken together, our results suggest that magenta and yellow morphs did not evolve through intermediate genotypes giving orange flowers, but that instead evolution followed the route defined by the U-shaped cloud. According to this view, the cloud represents a region of high fitness, allowing flower color to evolve without incurring major fitness costs. However, when genotypes, such as magenta and yellow morphs, from distant parts of the cloud meet, they can generate progeny that lie outside the high fitness cloud, creating a barrier to exchange of flower color alleles. This would account for the observed steep cline at loci controlling color differences in the hybrid zone. A 2D slice through the U-shaped cloud, passing perpendicularly through its two arms, would yield an adaptive landscape with two separate peaks. The cloud therefore represents a high fitness path between what might otherwise seem like distinct peaks, showing how higher dimensional representations allow adaptive continuity and incompatibility to be more easily reconciled (2).

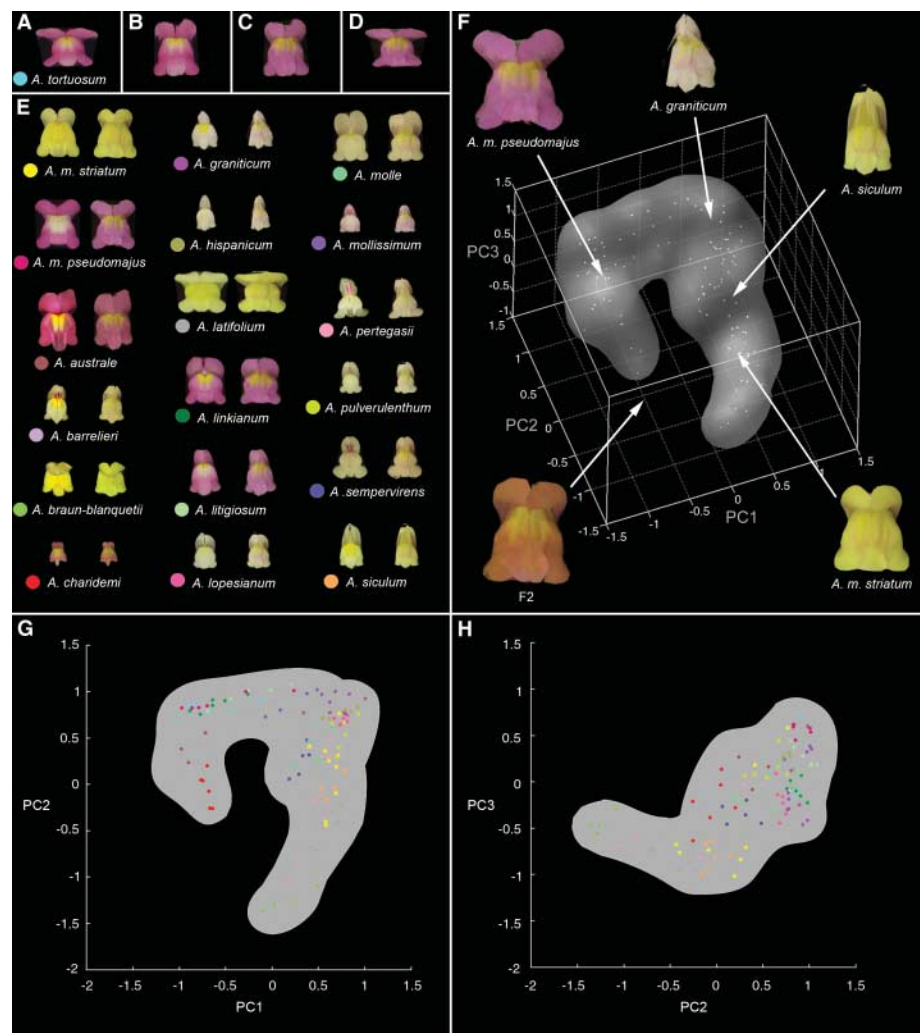


Fig. 4. *Antirrhinum* species placed in 3D genotypic space. (A) Mean *A. tortuosum* flower. (B) *A. tortuosum* flower warped to mean shape used to generate genotypic space (Fig. 1C). (C) Projection of (B) into genotypic space. (D) Image obtained when (C) is warped back to the mean *A. tortuosum* flower shape. (E) Projection of 19 *Antirrhinum* species into genotypic space. In each case, flower on the left shows the mean appearance, whereas flower on the right shows the appearance after projection into genotypic space [equivalent to (A) and (D) for each species]. (F) Cloud obtained for flowers from 19 species represented in genotypic space. Each point shows the position of a single flower projected into genotypic space. Examples of flowers from different positions in the genotypic space are illustrated. (G and H) Two different 2D projections of the cloud, with each species color-coded as in (E).

References and Notes

1. S. Wright, in Vol. 1 of *Proceedings of the Sixth Annual Congress of Genetics*, D. F. Jones, Ed. (Genetics Society of America, Austin, TX, 1932), p. 356–366.
2. S. Gavrilets, *Fitness Landscapes and the Origin of Species*, S. Levin, H. Horn, Eds., no. 41 of *Monographs in Population Biology* (Princeton Univ. Press, Princeton, NJ, 2004).
3. S. Gavrilets, *Trends Ecol. Evol.* **12**, 307 (1997).
4. W. Rothmaler, *Taxonomische Monographie der Gattung Antirrhinum* (Akademie-Verlag, Berlin, 1956).
5. D. A. Webb, in *Flora Europaea*, T. Tutin et al., Eds. (Cambridge Univ. Press, Cambridge, 1972), vol. 3.

6. D. Sutton, *A Revision of the Tribe Antirrhineae* (Oxford Univ. Press, Oxford, 1988).
7. I. Mateu-Andres, J. G. Segarra-Moragues, *Ann. Bot. (Lond.)* **92**, 647 (2003).
8. P. Vargas, J. A. Rosselló, R. Oyama, J. Güemes, *Plant Syst. Evol.* **249**, 151 (2004).
9. Z. Schwarz-Sommer, B. Davies, A. Hudson, *Nat. Rev. Genet.* **4**, 657 (2003).
10. T. Gubitz, A. Caldwell, A. Hudson, *Mol. Biol. Evol.* **20**, 1537 (2003).
11. J. Hackbarth, P. Michaelis, G. Scheller, *Z. Indukt. Abstammungs- Vererbungslehre* **80**, 1 (1942).
12. H. Stubbe, *Genetik und Zytologie von Antirrhinum L. sect. Antirrhinum* (Veb Gustav Fischer Verlag, Jena, Germany, 1966).
13. K. Schwinn *et al.*, *Plant Cell* **18**, 831 (2006).
14. E. Baur, *Bibl. Genet.* **4**, 1 (1924).
15. G. W. Horgan, *Comput. Electron. Agric.* **31**, 169 (2001).
16. T. F. Cootes, G. J. Edwards, C. J. Taylor, *IEEE Trans. Pattern Anal. Mach. Intell.* **23**, 681 (2001).
17. N. B. Langlade *et al.*, *Proc. Natl. Acad. Sci. U.S.A.* **102**, 10221 (2005).
18. N. H. Barton, G. M. Hewitt, *Annu. Rev. Ecol. Syst.* **16**, 113 (1985).
19. N. H. Barton, B. O. Bengtsson, *Heredity* **57**, 357 (1986).
20. D. Luo *et al.*, *Cell* **99**, 367 (1999).
21. E. S. Coen, R. Carpenter, C. Martin, *Cell* **47**, 285 (1986).
22. W. S. Moore, J. T. Price, in *Hybrid Zones and the Evolutionary Process*, R. G. Harrison, Ed. (Oxford Univ. Press, Oxford, 1993), pp. 196–225.
23. D. W. Schemske, H. D. Bradshaw Jr., *Proc. Natl. Acad. Sci. U.S.A.* **96**, 11910 (1999).
24. L. Chittka, J. D. Thomson, Eds., *Cognitive Ecology of Pollination* (Cambridge Univ. Press, Cambridge, 2001).
25. H. D. Bradshaw Jr., D. W. Schemske, *Nature* **426**, 176 (2003).
26. We thank C. Martin and J. Venail for providing the *ROS* sequence before publication; M. Burrus, L. Copsy, J. Bowers, C. Cazettes-Vicedo, and Z.-L. Liu for their help with carrying out genotyping and genetics; M. Bernardet, M. Cruzan, and J. Leneveu for their help in the field; and G. Hewitt for helping to initiate this project. This research was funded by grants from the Biotechnology and Biological Sciences Research Council, UK. Sequences are deposited in GenBank; accession numbers DQ866629 to DQ866657 for *ROSEA1*, DQ866658 to DQ866676 for *PALLIDA*, and DQ866677 to DQ866701 for *DICHOTOMA*.

Supporting Online Material

www.sciencemag.org/cgi/content/full/313/5789/963/DC1
Materials and Methods
Figs. S1 to S3
Tables S1 and S2
References

25 April 2006; accepted 21 July 2006
10.1126/science.1129161

Plant Genotypic Diversity Predicts Community Structure and Governs an Ecosystem Process

Gregory M. Crutsinger,^{1*} Michael D. Collins,¹ James A. Fordyce,¹ Zachariah Gompert,² Chris C. Nice,² Nathan J. Sanders¹

Theory predicts, and recent empirical studies have shown, that the diversity of plant species determines the diversity of associated herbivores and mediates ecosystem processes, such as aboveground net primary productivity (ANPP). However, an often-overlooked component of plant diversity, namely population genotypic diversity, may also have wide-ranging effects on community structure and ecosystem processes. We showed experimentally that increasing population genotypic diversity in a dominant old-field plant species, *Solidago altissima*, determined arthropod diversity and community structure and increased ANPP. The effects of genotypic diversity on arthropod diversity and ANPP were comparable to the effects of plant species diversity measured in other studies.

Ecological theory (1, 2) and field experiments (3, 4) have revealed a positive relationship between the diversity of plant species and the diversity of associated consumers. At least two mechanisms might explain this pattern. First, because approximately 90% of herbivorous insects exhibit some degree of host specialization (5), as plant species richness increases, so should the number of associated herbivore species. This resource specialization hypothesis has some theoretical support (1, 2, 6). Second, if aboveground net primary productivity (ANPP) increases as plant species richness increases (7), then more herbivore individuals, and therefore more species, will be supported by increases in available energy (this has been called the more individuals hypothesis) (8). An increase in the number of herbivore species by either of these mechanisms should support more predator species (9). Recent studies have

shown that population genotypic diversity, like plant species diversity, can have extended consequences for communities and ecosystems (10–14). However, no studies to date have explicitly linked intraspecific genotypic diversity, the structure of associated communities, and the potential mechanisms driving these patterns, such as energy availability. This paucity of studies exists despite numerous calls for such research within the literature regarding biodiversity-ecosystem function (7, 15). We tested whether host-plant genotypic diversity determines the structure of associated arthropod communities and governs an ecosystem process, ANPP, that influences arthropod species richness.

We manipulated the plot-level genotypic diversity (the number of genotypes per plot) of *Solidago altissima*, tall goldenrod, a common perennial plant throughout eastern North America. Twenty-one *S. altissima* ramets were collected from local *S. altissima* patches growing in fields near the study site, and each ramet was identified as a unique genotype by means of amplified fragment length polymorphism. From these 21 genotypes, we established 63 1-m² experimental plots, each containing 12 individ-

uals and 1, 3, 6, or 12 randomly selected genotypes, mimicking the densities and levels of genotypic diversity found in natural patches of similar size. We censused arthropods on every ramet in each plot five times over the course of the growing season. In total, we counted 36,997 individuals of ~136 species. We estimated ANPP at the peak of the growing season using nondestructive allometric techniques (16).

Total cumulative arthropod species richness increased with plant genotypic diversity. The number of arthropod species was, on average, 27% greater in 12-genotype plots than in single-genotype plots (Fig. 1), indicating that plant genotypic diversity was an important determinant of arthropod diversity. When we examined the effects of genotypic diversity on community structure, we found that herbivore species richness (Fig. 2B) and predator richness (Fig. 2A) also increased with increasing genotypic diversity. The effects of genotypic diversity on arthropod communities were nonadditive (Fig. 1). That is, total arthropod richness and herbivore and predator richness were all greater in the 6- and 12-genotype plots than would be predicted by summing the number of arthropod species associated with the corresponding genotypes grown in monoculture ($P < 0.01$).

ANPP also increased with plant genotypic diversity and was 36% greater in 12-genotype plots than in single-genotype plots (Fig. 2C). The effect of genotypic diversity on ANPP could be due to increased niche complementarity (mixed genotypes used available resources more completely or mixed genotypes facilitated one another, thereby increasing ANPP in mixtures) (7, 15) or to sampling or selection effects (increased ANPP caused by randomly assembled mixtures having a higher probability of containing highly productive genotypes) (17). Using standard techniques (18) we found that selection effects were highly variable and were not significantly different from zero ($P > 0.60$ for all treatments), indicating that highly productive genotypes do not dominate in mixtures and drive observed increases in ANPP. Selection

¹Department of Ecology and Evolutionary Biology, University of Tennessee, Knoxville, TN 37996, USA. ²Department of Biology, Texas State University, San Marcos, TX 78666, USA.

*To whom correspondence should be addressed. E-mail: gcrutsin@utk.edu

Supporting online material

Materials and Methods.

Plant Material: Wild type (JI:7) and *sulf inc* (JI:57) stocks were from the collection at the John Innes Centre, Norwich, UK. The *INC* locus encodes an anthocyanin biosynthetic enzyme (*SI*). Seed for *ros^{dor}* was provided by C. Martin (S2). Samples of leaf material and seed were collected from wild accessions between 1999 and 2003. Sampling of the hybrid zone site was conducted in 2002. Species nomenclature is according to Rothmaler (S3).

Sequence analysis: Genomic DNA was prepared from leaf tissue with the DNeasy Plant Mini kit (Qiagen) in accordance with the manufacturer's instructions. Primers were designed to amplify by PCR genomic regions of *ROSI* (GenBank accession: DQ275529), *PAL* (GenBank accession: X15536) and *DICH* (GenBank accession: AF199465). Primer sequences (5'-3') were as follows: *ROSI* TGTGTCACCTTAGAGTTAC and TCATCTCTCGAAAACCGACC; *PAL* TTCGTGCAACTGTTGCTGAT and TCCGATCATTCTTTCTTGAGG; *DICH* TAGCAAACCCCTTGATTGGC and TATGCTGATCCAAAATGGCA. Thermal cycling conditions were: 94°C for 2 min; 35 cycles of 94°C for 1 min, 55°C for 2 min, 72°C for 2 min; final extension at 94°C for 7 min. PCR products were purified from agarose gels using the QiaQuick gel extraction kit (Qiagen) and cloned into the pGEM-T Easy vector (Promega). Bi-directional sequencing of plasmid DNA using BigDye version 3.0 (Applied Biosystems) with primers flanking the multiple cloning site was performed on a single clone from each individual (unless PCR products of different sizes were detected, in which case one clone from each band was sequenced). An internal sequencing primer (5'-3') AAATGAAATGAAAGGACAGAT was also used to obtain complete sequence for the 1.0-1.2kb *ROSI* PCR product. Sequence alignments were generated using ClustalW (S4) and adjusted manually, where required (see detailed alignments below). Phylogenetic analysis by maximum parsimony (Dnapars) was performed with PHYLIP version 3.65 (S5). Gaps were incorporated in the analysis as a fifth character state, with indels of contiguous bases coded as a single event. Sequence input order was jumbled 5 times for each analysis. Bootstrap support was generated from 100 replicates.

Genotyping assays: Multiplex PCR assays were developed for genotyping at the *ROSI*, *PAL* and *DICH* loci using the Qiagen Multiplex PCR kit. Haplogroup-specific primers were used in combination with a common primer to generate products of different sizes that could be resolved on 1.5% agarose gels. Primer sequences are shown in Table S2. PCR reactions were carried out in a 10µl total volume containing 5µl 2x Qiagen master mix, 0.2µM each primer and ~80ng genomic DNA. Thermal cycling conditions were: 95°C for 15 minutes; 30 cycles of 94°C for 30 seconds, 57°C for 1 minute 30 seconds and 72°C extension for 1 minute 30 seconds; a final extension step of 72°C for 10 minutes.

Phenotype and allele frequencies analysis in the hybrid zone: The geographic distance used in the hybrid zone transect is the longitudinal distance from the westernmost subpopulation after projection on a line defined by the linear regression of the UTM-coordinates of each subpopulation. The mean values of color scores (usually 9 to 15 plants per sub-population) were normalized from 0 to 1. Magenta scores were confirmed by measuring anthocyanin content spectroscopically in flowers from F2 populations between the two morphs. Differences in magenta color score were strongly associated with variation in anthocyanin content ($F_{1,549}=3023$, $P<0.0001$; adj. $R^2=0.85$). We fitted a sigmoid cline to transect data using a tanh model (yellow: $f(x) = (1 + \tanh[2(C-x)/W])/2$, magenta and *ROSI*: $f(x) = (1 + \tanh[2(x-C)/W])/2$, where x and $f(x)$ are variables corresponding to a location along the transect and sub-population means of the character, respectively, while C and W stands for the position of the cline center and

width, respectively. Curves were fitted with a least-mean-square routine in MATLAB. The fitting results with the 95% confidence boundaries were: yellow color score: centre (C) = 12.56 ± 0.10 km, width (W) = 1.20 ± 0.38 km (adj. $R^2 = 0.8891$); magenta color score: centre = 12.70 ± 0.05 km, width = 0.44 ± 0.18 km (adj. $R^2 = 0.9115$); *ROSI* allele frequency: centre = 12.66 ± 0.04 km, width = 0.52 ± 0.12 km (adj. $R^2 = 0.9719$)(S6). To assess concordance between *ROSI* frequency and magenta color clines, we regressed subpopulation mean score for magenta color on *ROSI* allele frequencies(S7). This regression showed a very strong linear relationship ($P < 0.0001$; adj. $R^2 = 0.9647$). Quadratic term was non-significant ($P > 0.05$) and cubic term marginally significant ($P = 0.016$) but explaining only 0.4% more variation than the linear model (adj. $R^2 = 0.9683$), leading us to conclude that *ROSI* and magenta color clines were highly concordant.

Image analysis: Front photographs of flowers were taken in comparable light conditions with a Kodak Pro14N camera resulting in standard RGB color space images. A flower point model template was created in MATLAB, using the ‘Point Model Editor’ in the ‘AAM Toolbox’ package, available on request and from:

<http://www.cmp.uea.ac.uk/Research/cbg/downloads.htm>.

The 93 points of this template captured the overall flower shape. On the basis of these template landmarks, corresponding points were placed on the different populations and species flowers. This allowed us to calculate a mean flower shape from 4 genotypes in the F2 and to warp the corresponding images to this identical shape, encapsulating about 100,000 pixels. A statistical model of appearance was built using PCA from the RGB values of the 4 warped images(S8) (‘Stats Model Gen.’ in the ‘AAM Toolbox’). The three resulting axes capture the variation controlled by ROS, EL and SULF, and define a genotypic color space for flowers. To compare color intensity and pattern between the *Antirrhinum* flowers, we warped every image to the mean F2 shape and projected the warped flower color onto the genotypic space. For Fig.4E, 3-9 flowers were used to generate means for each species.

To create an outer surface enclosing the points in the species cloud Ω , we created a 3D grid which we call Φ . For each point p in Φ we calculate the mean distance δ to the 2 nearest points in Ω . We then create a scalar field by assigning a value to every point p that is inversely proportional to its δ . We display an isosurface for this field to generate a 2D surface embedded in 3D space that encloses points in Ω . To help visualise the geometry of the generated surface, a light source was placed in the 3D space to simulate highlights and shadows.


```

*           440           *           460           *           480           *           500           *           520           *
A.m.p.01 : ----- : -
A.m.p.02 : ----- : -
A.m.p.03 : ----- : -
A.m.p.04 : ----- : -
A.m.p.05 : ----- : -
A.m.p.06 : TGGGCGGGTTGTCGTTAAAAATATGACTATACTCAAACCTTTGCGGGTTACCAATTTTTCAACCCGAGTTAAAAACTAAACCATGCGGGTTGCGGGTTGGGCGAGTCG : 523
A.m.p.07 : TGGGCGGGTTGTCGTTAAAAATATGACCATACTCAAACCTTTGCGGGTTACCAATTTTTCAACCCGAGTTAAAAACTAAACCATGCGGGTTGCGGGTTGGGCGAGTCG : 523
A.m.p.08 : TGGGCGGGTTGTCGTTAAAAATATGACCATACTCAAATTTTTCGCGGGTTACCAATTTTTCAACCCGAGTTAAAAGCTAAACCATGCGGGTTGCGGGTTGGGCGAGTCG : 522
A.m.p.09 : TGGGCGGGTTGTCGTTAAAAATATGACCATACTCAAATTTTTCGCGGGTTACCAATTTTTCAACCCGAGTTAAAAGCTAAACCATGCGGGTTGCGGGTTGGGCGAGTCG : 522
A.m.p.10 : TGGGCGGGTTGTCGTTAAAAATATGACCATACTCAAATTTTTCGCGGGTTACCAATTTTTCAACCCGAGTTAAAAGCTAAACCATGCGGGTTGCGGGTTGGGCGAGTCG : 522
A.m.p.11 : TGGGCGGGTTGTCGTTAAAAATATGACCATACTCAAATTTTTCGCGGGTTACCAATTTTTCAACCCGAGTTAAAAGCTAAACCATGCGGGTTGCGGGTTGGGCGAGTCG : 522
A.m.p.12 : TGGGCGGGTTGTCGTTAAAAATATGACCATACTCAAATTTTTCGCGGGTTACCAATTTTTCAACCCGAGTTAAAAGCTAAACCATGCGGGTTGCGGGTTGGGCGAGTCG : 521
A.m.p.13 : TGGGCGGGTTGTCGTTAAAAATATGACCATACTCAAATTTTTCGCGGGTTACCAATTTTTCAACCCGAGTTAAAAGCTAAACCATGCGGGTTGCGGGTTGGGCGAGTCG : 522
A.m.p.14 : TGGGCGGGTTGTCGTTAAAAATATGACCATACTCAAATTTTTCGCGGGTTACCAATTTTTCAACCCGAGTTAAAAGCTAAACCATGCGGGTTGCGGGTTGGGCGAGTCG : 521
A.m.p.15 : TGGGCGGGTTGTCGTTAAAAATATGACCATACTCAAATTTTTCGCGGGTTACCAATTTTTCAACCCGAGTTAAAAGCTAAACCATGCGGGTTGCGGGTTGGGCGAGTCG : 521
A.m.s.01 : ----- : -
A.m.s.02 : ----- : -
A.m.s.03 : ----- : -
A.m.s.04 : ----- : -
A.m.s.05 : ----- : -
A.m.s.06 : ----- : -
A.m.s.07 : ----- : -
A.m.s.08 : ----- : -
A.m.s.09 : ----- : -
A.m.s.10 : ----- : -
A.m.s.11 : ----- : -
A.m.s.12 : ----- : -
A.m.s.13 : ----- : -
A.l. : ----- : -

```

```

540          *          560          *          580          *          600          *          620          *          640
A.m.p.01 : -----TGATCTAGCCATAAAAAAGCCTATATAAAACCCGTGCAAATTTTCGCTCAAGGGGTACTCAATA : 439
A.m.p.02 : -----TGATCTAGCCATAAAAAAGCCTATATAAAACCCGTGCAAATTTTCGCTCAAGGGGTACTCAATA : 439
A.m.p.03 : -----TGATCTAGCCATAAAAAAGCCTATATAAAACCCGTGCAAATTTTCGCTCAAGGGGTACTCAATA : 439
A.m.p.04 : -----TGATCTAGCCATAAAAAAGCCTATATAAAACCCGTGCAAATTTTCGCTCAAGGGGTACTCAATA : 439
A.m.p.05 : -----TGATCTAGCCATAAAAAAGCCTATATAAAACCCGTGCAAATTTTCGCTCAAGGGGTACTCAATA : 439
A.m.p.06 : GGTTTTGACGGGTCGGGCGGATCGGGCGGGTCATGAACACCCCTAGGCTACAGCCATAAAAAAGCCTATTTAAACCCGTGAAAGTTTCGCTCAAGGGGTACTCATT : 630
A.m.p.07 : GGTTTTGACGGGTCGGGCGGATCGGGCGGGTCATGAACACCCCTAGGCTACAGCCATAAAAAAGCCTATTTAAACCCGTGAAAGTTTCGCTCAAGGGGTACTCATT : 630
A.m.p.08 : GGTTTTGACGGGTCGGGCGGATCGGACGGGTCATGAACACCCCTAGGCTACAGCCATAAAAAAGCCTATTTAAACCCGTGAAAGTTTCGCTCAAGGGGTACTCATT : 629
A.m.p.09 : GGTTTTGACGAGTCTGGGCGGATCGGACGGGTCATGAACACCCCTAGGCTACAGCCATAAAAAAGCCTATTTAAACCCGTGAAAGTTTCGCTCAAGGGGTACTCATT : 629
A.m.p.10 : GGTTTTGACGGGTCGGGCGGATCGGACGGGTCATGAACACCCCTAGGCTACAGCCATAAAAAAGCCTATTTAAACCCGTGAAAGTTTCGCTCAAGGGGTACTCATT : 629
A.m.p.11 : GGTTTTGACGGGTCGGGCGGATCGGACGGGTCATGAACACCCCTAGGCTACAGCCATAAAAAAGCCTATTTAAACCCGTGAAAGTTTCGCTCAAGGGGTACTCATT : 629
A.m.p.12 : GGTTTTGATGGGTTTGGGCGGATCGAACGGGTCATGAACACCCCTAGGCTACAGCCATAAAAAAGCCTATTTAAACCCGTGAAAGTTTCGCTCAAGGGGTACTCATT : 627
A.m.p.13 : GGTTTTGACGGGTCGGGCGGATCGGACGGGTCATGAACACCCCTAGGCTACAGCCATAAAAAAGCCTATTTAAACCCGTGAAAGTTTCGCTCAAGGGGTACTCATT : 629
A.m.p.14 : GGTTTTGACGGGTCGGGCGGATCGAACGGGTCATGAACACCCCTAGGCTACAGCCATAAAAAAGCCTATTTAAACCCGTGAAAGTTTCGCTCAAGGGGTACTCATT : 628
A.m.p.15 : GGTTTTGACGGGTCGGGCGGATCGAACGGGTCATGAACACCCCTAGGCTACAGCCATAAAAAAGCCTATTTAAACCCGTGAAAGTTTCGCTCAAGGGGTACTCATT : 628
A.m.s.01 : -----CTACAGCCATAAAAAAGCCTATTTAAATCCGTGAAAGTTTCGCTTAAGGGGTACTCATT : 455
A.m.s.02 : -----CTACAGCCATAAAAAAGCCTATTTAAATCCGTGAAAGTTTCGCTTAAGGGGTACTCATT : 455
A.m.s.03 : -----CTACAGCCATAAAAAAGCCTATTTAAATCCGTGAAAGTTTCGCTTAAGGGGTACTCATT : 455
A.m.s.04 : -----CTACAGCCATAAAAAAGCCTATTTAAATCCGTGAAAGTTTCGCTTAAGGGGTACTCATT : 455
A.m.s.05 : -----CTACAGCCATAAAAAAGCCTATTTAAATCCGTGAAAGTTTCGCTTAAGGGGTACTCATT : 455
A.m.s.06 : -----CTACAGCCATAAAAAAGCCTATTTAAATCCGTGAAAGTTTCGCTTAAGGGGTACTCATT : 455
A.m.s.07 : -----CTACAGCCATAAAAAAGCCTATTTAAATCCGTGAAAGTTTCGCTTAAGGGGTACTCATT : 455
A.m.s.08 : -----CTACAGCCATAAAAAAGCCTATTTAAATCCGTGAAAGTTTCGCTTAAGGGGTACTCATT : 455
A.m.s.09 : -----CTACAGCCATAAAAAAGCCTATTTAAATCCGTGAAAGTTTCGCTTAAGGGGTACTCATT : 455
A.m.s.10 : -----CTACAGCCATAAAAAAGCCTATTTAAATCCGTGAAAGTTTCGCTTAAGGGGTACTCATT : 455
A.m.s.11 : -----CTACAGCCATAAAAAAGCCTATTTAAATCCGTGAAAGTTTCGCTTAAGGGGTACTCATT : 455
A.m.s.12 : -----CTACAGCCATAAAAAAGCCTATTTAAATCCGTGAAAGTTTCGCTTAAGGGGTACTCATT : 455
A.m.s.13 : -----CTACAGCCATAAAAAAGCCTATTTAAATCCGTGAAAGTTTCGCTTAAGGGGTACTCATT : 455
A.l. : -----CTACAGCCATAAAAAAGTCTACAGCCATAAAAAAGCCTATTTAAATCCGTGAAAGTTTCGCTTAAGGGGTACTCATT : 471

```



```

          540          *          560          *          580
A.m.p.01 : ATTACAGTAACTTTACCTCACAGTCCAACCAGCTATGTGCCATTTTGGATCAGCATA : 548
A.m.p.02 : ATTACAGTAACTTTACCTCACAGTCCAACCAGCTATGTGCCATTTTGGATCAGCATA : 551
A.m.p.03 : ATTACAGTAACTTTACCTCACAGTCCAACCAGCTATGTGCCATTTTGGATCAGCATA : 548
A.m.p.04 : ATTACAGTAACTTTACCTCACAGTCCAACCAGCTATGTGCCATTTTGGATCAGCATA : 551
A.m.p.05 : ATTACAGTAACTTTACCTCACAGTCCAACCAGCTATGTGCCATTTTGGATCAGCATA : 548
A.m.p.06 : ATTACAGTAACTTTACCTCACAGTCCAACCAGCTATGTGCCATTTTGGATCAGCATA : 551
A.m.p.07 : ATTACAGTAACTTTACCTCACAGTCCAACCAGCTATGTGCCATTTTGGATCAGCATA : 548
A.m.p.08 : ATTACAGTAACTTTACCTCACAGTCCAACCAGCTATGTGCCATTTTGGATCAGCATA : 551
A.m.p.09 : ATTACAGTAACTTTACCTCACAGTCCAACCAGCTATGTGCCATTTTGGATCAGCATA : 548
A.m.p.10 : ATTACAGTAACTTTACCTCACAGTCCAACCAGCTATGTGCCATTTTGGATCAGCATA : 548
A.m.p.11 : ATTACAGTAACTTTACCTCACAGTCCAACCAGCTATGTGCCATTTTGGATCAGCATA : 548
A.m.s.01 : ATTACAGTAACTTTACCTCACAGTCCAACCAGCTATGTGCCATTTTGGATCAGCATA : 548
A.m.s.02 : ATTACAGTAACTTTACCTCACAGTCCAACCAGCTATGTGCCATTTTGGATCAGCATA : 548
A.m.s.03 : ATTACAGTAACTTTACCTCACAGTCCAACCAGCTATGTGCCATTTTGGATCAGCATA : 548
A.m.s.04 : ATTACAGTAACTTTACCTCACAGTCCAACCAGCTATGTGCCATTTTGGATCAGCATA : 548
A.m.s.05 : ATTACAGTAACTTTACCTCACAGTCCAACCAGCTATGTGCCATTTTGGATCAGCATA : 581
A.m.s.06 : ATTACAGTAACTTTACCTCACAGTCCAACCAGCTATGTGCCATTTTGGATCAGCATA : 551
A.m.s.07 : ATTACAGTAACTTTACCTCACAGTCCAACCAGCTATGTGCCATTTTGGATCAGCATA : 548
A.m.s.08 : ATTACAGTAACTTTACCTCACAGTCCAACCAGCTATGTGCCATTTTGGATCAGCATA : 548
A.m.s.09 : ATTACAGTAACTTTACCTCACAGTCCAACCAGCTATGTGCCATTTTGGATCAGCATA : 548
A.m.s.10 : ATTACAGTAACTTTACCTCACAGTCCAACCAGCTATGTGCCATTTTGGATCAGCATA : 551
A.m.s.11 : ATTACAGTAACTTTACCTCACAGTCCAACCAGCTATGTGCCATTTTGGATCAGCATA : 551
A.m.s.12 : ATTACAGTAACTTTACCTCACAGTCCAACCAGCTATGTGCCATTTTGGATCAGCATA : 551
A.m.s.13 : ATTACAGTAACTTTACCTCACAGTCCAACCAGCTATGTGCCATTTTGGATCAGCATA : 548
A.l. : ATTACAGTAACTTTACCTCACAGTCCAACCAGCTATGTGCCATTTTGGATCAGCATA : 551

```

Table S1 Population details and distances from hybrid zone

Morph	Code	Latitude (°N)	Longitude (°E)	Distance from Hybrid Zone (km)
<i>A. m. pseudomajus</i>	AUT	43.33	1.51	122
<i>A. m. pseudomajus</i>	BAG	43.10	2.98	113
<i>A. m. pseudomajus</i>	BAN	42.49	3.12	87
<i>A. m. pseudomajus</i>	BED	42.86	1.57	74
<i>A. m. pseudomajus</i>	CAB	43.35	2.46	119
<i>A. m. pseudomajus</i>	CHI	42.77	1.86	54
<i>A. m. pseudomajus</i>	FLO	43.17	2.47	100
<i>A. m. pseudomajus</i>	POR	42.21	1.54	47
<i>A. m. pseudomajus</i>	SAL	42.23	1.74	31
<i>A. m. pseudomajus</i>	UNA	42.76	1.79	55
<i>A. m. striatum</i>	AND	42.57	1.59	50
<i>A. m. striatum</i>	CAM	42.80	1.92	55
<i>A. m. striatum</i>	CAS	42.77	2.78	76
<i>A. m. striatum</i>	JOS	42.26	1.64	38
<i>A. m. striatum</i>	LUC	42.97	2.26	74
<i>A. m. striatum</i>	LYS	42.83	2.20	57

Table S2: Primer sequences for PCR genotyping assays

Locus	Primer	Sequence (5'→3')	Function
<i>ROSI</i>	RG4	CAGGTTACAGTAGGGTGTTCG	<i>ROS-Ma</i> forward primer
	RG6	CAAAGGGGTGATCTAGCC	<i>ROS-Mb</i> forward primer
	RG1	GGACAGATGATTAATTACATGA	<i>ROS-Y</i> forward primer
	RR21	TCATCTCTCGAAAACCGACC	Common reverse primer
<i>PAL</i>	PG1A	GAGAGTCATGACTTGAGTCTATTG	<i>PAL-A</i> forward primer
	PG2B	CCTTAATCGTATAAGAATTTCCAAC	<i>PAL-B</i> forward primer
	PALR1	TCCGATCATTCTTGGAGG	Common reverse primer
<i>DICH*</i>	DG1	TCAGGTCCCTCAACTAATTATG	<i>DICH-A</i> forward primer
	DG2	TCAGGTCCCTCAAGCTATGAA	<i>DICH-B</i> forward primer
	DICHR1	TATGCTGATCCAAAATGGCA	Common reverse primer
	DICHF1	TAGCAAAACCCCTTGATTGGC	Positive control forward primer

Two separate multiplex PCR reactions (primer DG1 or DG2 plus DICHF1 and DICHR1) were carried out for *DICH* as the sequence variants could not be distinguished by size. Genotype was inferred from the combined results of the two reactions.

References

- S1. C. Martin, A. Prescott, S. Mackay, J. Bartlett, E. Vrijlandt, *Plant Journal* 1, 37 (1991).
- S2. K. Schwinn *et al.*, *Plant Cell* 18, 831 (2006).
- S3. W. Rothmaler, *Taxonomische Monographie der Gattung Antirrhinum*. (Akademie-Verlag, Berlin, 1956).
- S4. R. Chenna *et al.*, *Nucleic Acids Res* 31, 3497 (2003).
- S5. J. Felsenstein. (Distributed by the author. Department of Genome Sciences, University of Washington, Seattle., 2005).
- S6. N. H. Barton, B. O. Bengtsson, *Heredity* 57, 357 (1986).
- S7. N. H. Barton, G. M. Hewitt, *Annual Review of Ecology and Systematics* 16, 113 (1985).
- S8. G. W. Horgan, *Computers and Electronics in Agriculture* 31, 169 (2001).

scientific controversy distract us from attending to the needs of trauma victims (10). But criticism is vital for any scientific field, and discovering new facts, however politically incorrect they may seem, provides the best basis for helping victims. The new study's conclusion that the NVVRS overestimated the rate of PTSD by 40% will upset some people. Yet by increasing the accuracy of our prevalence estimates, Dohrenwend *et al.* have performed a valuable service. Advocacy for victims must rest on the best science possible.

References

1. B. P. Dohrenwend *et al.*, *Science* **313**, 978 (2006).
2. Centers for Disease Control Vietnam Experience Study, *J. Am. Med. Assoc.* **259**, 2701 (1988).
3. R. A. Kulka, W. E. Schlenger, J. A. Fairbank, R. L. Hough, B. K. Marmar, D. S. Weiss, *Trauma and the Vietnam War Generation: Report of Findings from the National Vietnam Veterans Readjustment Study* (Brunner/Mazel, New York, 1990).
4. B. Shephard, *A War of Nerves: Soldiers and Psychiatrists in the Twentieth Century* (Harvard Univ. Press, Cambridge, MA, 2001).
5. E. T. Dean Jr., *Shook Over Hell: Post-traumatic Stress, Vietnam, and the Civil War* (Harvard Univ. Press, Cambridge, MA, 1997).
6. D. H. Marlowe, *Psychological and Psychosocial Consequences of Combat and Deployment with Special Emphasis on the Gulf War* (RAND, Santa Monica, CA, 2001).
7. B. C. Frueh *et al.*, *Brit. J. Psychiat.* **186**, 467 (2005).
8. Department of Veterans Affairs, Office of the Inspector General, *Review of State Variances in VA Disability Compensation Payments (Report #05-00765-137)* (2005); www.va.gov/foia/err/standard/requests/ig.html.
9. R. J. McNally, *Remembering Trauma* (Harvard Univ. Press, Cambridge, MA, 2003).
10. D. Kilpatrick, *Traumatic StressPoints* **20**, 2 (2006); www.istss.org.

10.1126/science.1132242

EVOLUTION

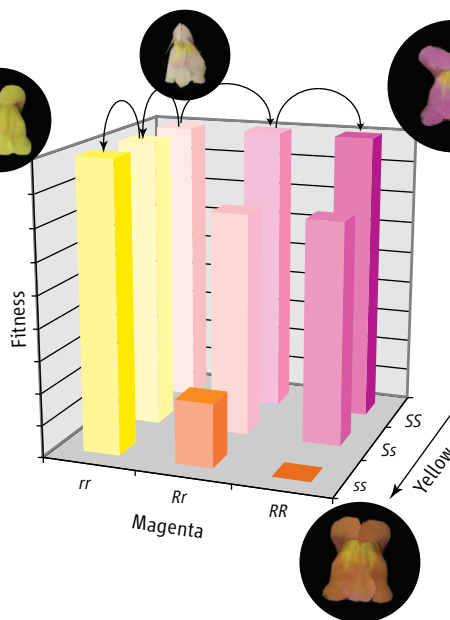
Traversing the Adaptive Landscape in Snapdragons

Elena M. Kramer and Kathleen Donohue

How does one species become two species? Species appear to be stable, adapted entities reproductively isolated from related species, but how did this isolation appear? We can view species in terms of populations in an adaptive landscape—a topographical plot of fitness as a function of combinations of characteristics. Each species then sits on its own high ground, sporting adaptive characteristics (collectively, their phenotypes), while they tower over valleys of maladaptive phenotypes. Does this high ground represent isolated peaks, each species inhabiting one of them, or are the areas of high ground connected by an equally high ridge, long and circuitous though it may be?

Distinguishing between these two possibilities is fundamental to understanding speciation. With two isolated peaks, there is no way to get from one to the other except through great mutational leaps, tromping through a valley of low fitness, or waiting for the environment (the landscape itself) to change. In the alternative case, one can simply walk randomly along a ridge. The evolutionary mechanisms are very different between those two scenarios, including the roles of natural selection, drift, migration, and mutation. On page 963 of this issue, Whibley *et al.* provide evidence that speciation in snapdragons may have occurred through a walk along an adaptive ridge (1).

Since Wright first introduced the concept of the adaptive landscape in 1932 (2), it has



become one of the most important heuristic tools in evolutionary biology. The original formulation plotted fitness in a population as a function of the frequency of different forms of specific genes (alleles), resulting in a contoured landscape where the peaks represent local optima that correspond to a particular genotype. This concept was modified by Simpson (3) and Lande (4) to yield an alternate landscape that plots fitness as a function of phenotypic values, where the surface represents the relative fitness of particular phenotypes in a population. Given that many phenotypes are quite complex at the genetic level, however, the relationship between genotype and phenotype has often proven difficult to quantify. As Wright himself pointed out, the

The genetic changes that underlie adaptive evolution of species are not easy to determine. Snapdragon species with different flower colors that coexist in the Pyrenees offer a promising system for analyzing them.

Evolution along an adaptive ridge. Whibley *et al.* found three loci associated with floral color, two being tightly linked and virtually inherited as one. The diagram represents their results in terms of evolution of a two-gene system along a ridge that creates reproductive isolation between the subspecies. The z axis indicates the fitness of flowers with different colors, with orange being in the valley of low fitness and yellow and magenta along the ridge of high fitness. Arrows indicate stepwise changes from one genotype to another, starting with *rrSS*. One subspecies in their study had genotype *RRSS* and the other had *rrss* (where *R* = *ROS*, *S* = *SULF*). Other extant subspecies of snapdragon are expected to contain genotypes found along the ridge but not genotypes in the valley or slopes.

true adaptive landscape exists in thousands of dimensions, with many genes sometimes contributing to a single phenotype under selection. Thus, many authors have debated the true nature of an adaptive landscape: whether it is smooth or rugged, with many isolated peaks or few, with the highest level of adaptation represented by single points or by continuous ridges [see the review by Schluter (5)].

A classic model of speciation along an adaptive ridge is the Dobzhansky-Muller model. Imagine a population with individuals that have the two-locus (two-gene) genotype *rrSS* (where upper and lower case denote different alleles), and the population divides into two. In one population, a new *R* allele arises and replaces *r*, so the population now has genotype *RRSS*. In the other, a new *s* allele arises and replaces *S*, and the population has the genotype *rrss*. Note that the *R* allele has never occurred with the *s* allele during this

The authors are in the Department of Organismic and Evolutionary Biology, Harvard University, Cambridge, MA 02138, USA. E-mail: ekramer@oeb.harvard.edu

process. If the combination of R and s results in low fitness, then the two new populations would be reproductively isolated (their offspring would have low fitness because they would contain both R and s), even though neither population went through any stage of low fitness itself.

Whibley *et al.* provide a possible real-world example of this process (see the figure). The authors conducted a study of naturally hybridizing subspecies of *Antirrhinum majus*, a snapdragon. The yellow-flowered *A. m. striatum* and magenta-flowered *A. m. pseudomajus* form a narrow hybrid zone where their ranges meet in the Pyrenees. Whibley *et al.* were able to identify three loci that contribute significantly to the flower color differences between the two morphs. To further investigate the evolutionary interactions of the yellow and magenta floral forms, Whibley *et al.* combined an elegant digital color quantification technique with principal components analysis to define a phenotypic space for flower color. Although the F_2 (second generation and offspring of interbred hybrids) plants from a *striatum-pseudomajus* cross occupied a relatively large portion of the space, variation observed in natural subspecies was restricted to a narrower domain. In particular, an orange-colored form obtained in the F_2 crosses was never observed in natural populations. The authors suggest that this result reflects reduced fitness due to pollinator aversion and conclude that lowered fitness among the hybrids has helped to isolate the parental genotypes. Moreover, the seemingly disjunct yellow and magenta forms are found to occupy the extremes of a contiguous domain in genetically determined phenotypic space. If the maintenance of these colors in nature reflects their higher fitness, the connection between the two extremes can be interpreted as a route for the transition from yellow to magenta while avoiding the fitness valley represented by the orange genotypes. This connection can be thought of as an adaptive ridge in which the magenta/yellow domain of genotype space represents a continuous ridge of high fitness. Populations or species tend to evolve upward toward the ridge crest, resulting in a random distribution along the ridge. In this case, it appears that one defining feature of the ridge is that when two populations come into contact, their hybridization produces some phenotypes that “fall off” the ridge, resulting in lower fitness.

The current study is possible because the authors can make accurate predictions about the relationships between color and genotype, allowing the conversion between phe-

notypic and genotypic space. The genetic simplicity of the system makes it irresistible for actual tests of the Dobzhansky-Muller dynamic through measures of natural selection on the different genotypes. Note that an adaptive landscape describes the relationship between genotypes and fitness in a single environment. The model therefore would make the simple and testable prediction that all extant floral color genotype combinations would have comparable fitness across the entire geographical range of distribution, and all missing phenotypes (presumably those carrying the incompatible combination of R and s) would have equally low fitness across the range. The alternative hypothesis is that each color morph is locally adapted to its own local environment. Such measurements would address a fundamental question regard-

ing speciation, namely whether environment-independent genetic incompatibilities alone account for reproductive isolation between species that have diverged essentially through drift along a ridge, or whether divergent adaptation to different environments is the cause. In short, just what is the role of natural selection in speciation?

References

1. A. C. Whibley *et al.*, *Science* **313**, 963 (2006).
2. S. Wright, in *Proceedings of the Sixth International Congress of Genetics*, D. F. Jones, Ed. (Brooklyn Botanic Garden, Menasha, WI, 1932), vol. 1, pp. 356–366.
3. G. G. Simpson, *Tempo and Mode in Evolution* (Columbia Univ. Press, New York, 1944).
4. R. Lande, *Evolution* **33**, 402 (1979).
5. D. Schluter, *The Ecology of Adaptive Radiation* (Oxford Univ. Press, Oxford, 2000).

10.1126/science.1130958

ASTRONOMY

A Journey Through Time

Joseph Silk

Small variations in the temperature and density of matter just after the Big Bang are thought to have been the seeds for the galaxies we see today. This picture has been confirmed by observational evidence.

The cosmic microwave background radiation left over from the Big Bang provides a unique window on the very early universe. We believe now that galaxies formed as small variations in matter density evolved under the influence of gravity. If so, then the primordial fluctuations had to have a finite amplitude given the limited time available for fluctuation growth. An inevitable consequence is that temperature fluctuations must be generated in the cosmic microwave background. Recent observations of the background radiation confirm this picture of the gravity-induced growth of structure in the early universe.

The first predictions of cosmic temperature fluctuations were made in 1967 by Sachs and Wolfe (1). It was not until 1992 that NASA's Cosmic Background Explorer (COBE) verified, to within a factor of 2, the predicted effect (2). This is with hindsight also the prediction of the inflationary theory of cosmology of large-angular scale temperature fluctua-

tions generated in the first 10^{-36} s of the Big Bang. It was to take more than a decade, however, before the fine-scale anisotropy predictions (3, 4) associated with galaxy formation were confirmed (5).

Each time there was a major experimental improvement, the theoretical hurdle was raised as the predictions were refined. The ultimate prediction of temperature fluctuations arising from structure formation, made in 1984 (6, 7), was only 3 parts in 100,000, at an angular scale of about 30 arc min, and substantially lower on smaller angular scales. Eventually, ground-based and balloon-borne experiments provided strong confirmation of the elusive signal. But it was the release of first-year data from the Wilkinson Microwave Anisotropy Probe (WMAP) satellite in 2003 that provided the first high-precision measurements (8). Cosmology would never be the same again with the new refined measurements.

There were several dramatic results. The universe had to be flat, and at the critical density. Most of its mass-energy density was in the form of dark energy. One-third of the critical density was in nonbaryonic matter, and only 15% of that was in baryons (such as neutrons and protons). The primordial fluctua-

Enhanced online at
www.sciencemag.org/cgi/content/full/313/5789/925

The author is in the Department of Physics, University of Oxford, Oxford OX1 3RH, UK. E-mail: silk@astro.ox.ac.uk